QCD phase diagram

Alexei Bazavov

Michigan State University

December 14, 2017

in collaboration with
H.-T. Ding, P. Hegde, O. Kaczmarek, F. Karsch, E. Laermann,
Y. Maezawa, S. Mukherjee, H. Ohno, P. Petreczky, H. Sandmeyer,
P. Steinbrecher, C. Schmidt, S. Sharma, W. Soeldner, M. Wagner

Quantum Chromodynamics (QCD)

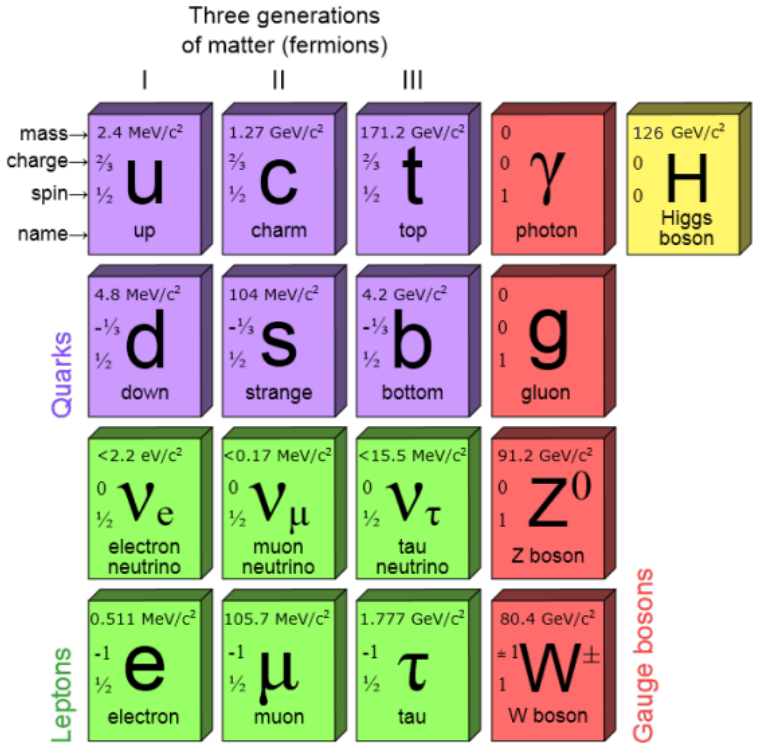

- Standard Model of Particle Physics: strong and electro-weak interactions

Quantum Chromodynamics (QCD)

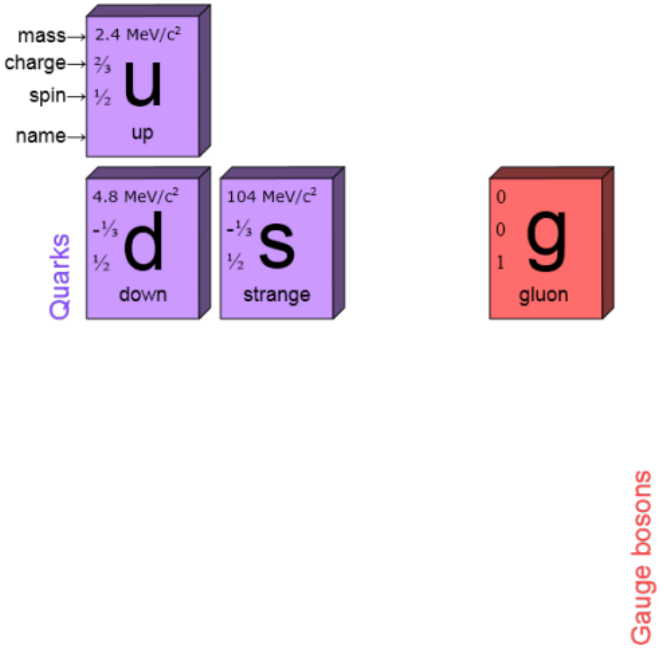

- Standard Model of Particle Physics: strong and electro-weak interactions
- Strong interactions: Quantum Chromodynamics (QCD)

Quantum Chromodynamics (QCD)

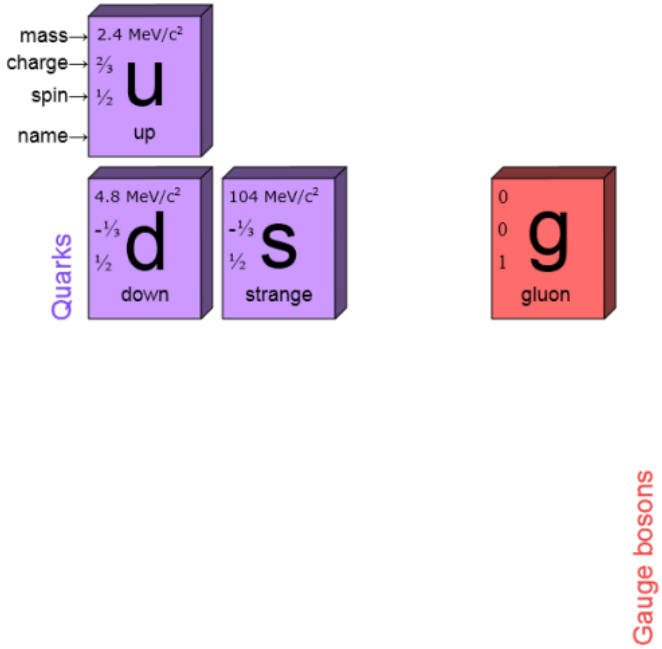

- Standard Model of Particle Physics: strong and electro-weak interactions
- Strong interactions: Quantum Chromodynamics (QCD)
- Confinement, chiral symmetry breaking

Quantum Chromodynamics (QCD)

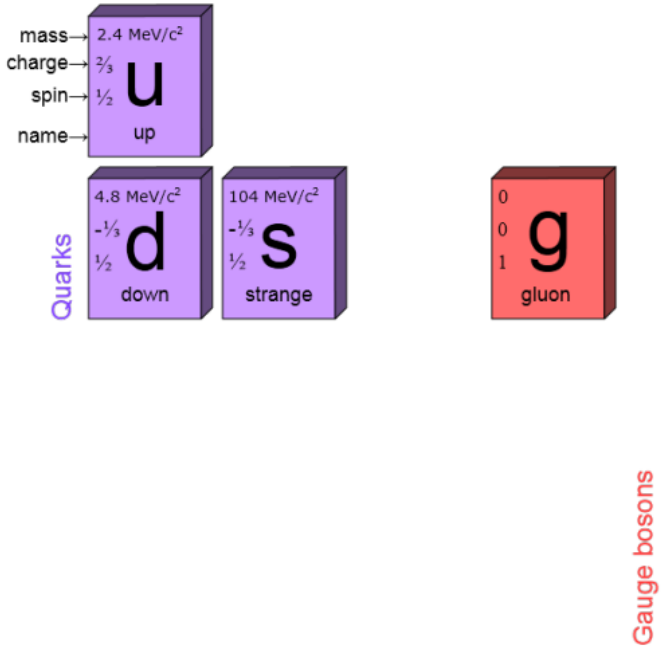

- Standard Model of Particle Physics: strong and electro-weak interactions
- Strong interactions: Quantum Chromodynamics (QCD)
- Confinement, chiral symmetry breaking
- Zero-temperature: properties of individual hadrons

Quantum Chromodynamics (QCD)

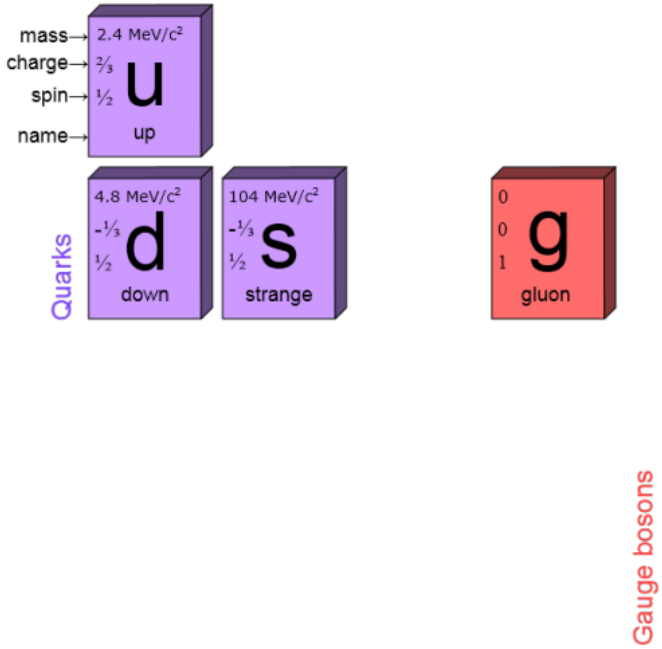

- Standard Model of Particle Physics: strong and electro-weak interactions
- Strong interactions: Quantum Chromodynamics (QCD)
- Confinement, chiral symmetry breaking
- Zero-temperature: properties of individual hadrons
- Finite-temperature: collective behavior, thermodynamics

Quantum Chromodynamics (QCD)

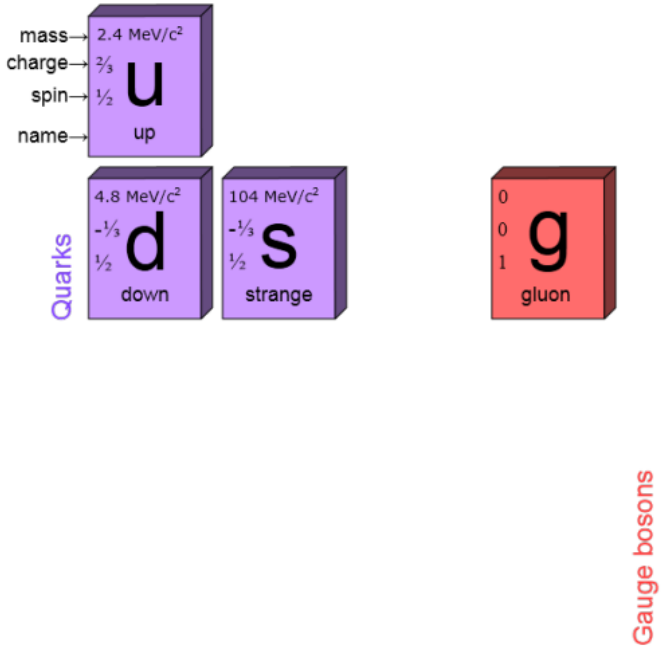

- Standard Model of Particle Physics: strong and electro-weak interactions
- Strong interactions: Quantum Chromodynamics (QCD)
- Confinement, chiral symmetry breaking
- Zero-temperature: properties of individual hadrons
- Finite-temperature: collective behavior, thermodynamics

- The QCD Lagrangian

$$\mathcal{L}_{QCD} = -\frac{1}{4} G^c_{\mu\nu} G^{\mu\nu,c} + \sum_{f=u,d,s} \bar{\psi}^c_f (i\gamma^\mu D^{cd}_\mu - m_f \delta^{cd}) \psi^d_f$$

QCD units of measure

$$
\begin{aligned}
1 \text{ eV} &= 1.6 \times 10^{-19} \text{ J} \\
1 \text{ MeV} &= 10^{6} \text{ eV} \\
1 \text{ GeV} &= 10^{9} \text{ eV} \\
1 \text{ fm} &= 10^{-15} \text{ m} \\
\hbar &= 1 \\
c &= 1 \\
1 &= \hbar c \simeq 200 \text{ MeV} \times 1 \text{ fm} \\
100 \text{ MeV} &\sim 10^{12} \text{ K} \\
\text{light quarks} &\sim \text{few MeV} \\
\text{proton} &\sim 1 \text{ GeV}
\end{aligned}
$$

Thermodynamics of QCD

Thermodynamics of QCD

- Gross, Wilczek (1973), Politzer (1973) – strong interactions weaken at high energies

Thermodynamics of QCD

- Gross, Wilczek (1973), Politzer (1973) – strong interactions weaken at high energies
- Cabbibo, Parisi (1975), Collins, Perry (1975) conjectured the phase structure:

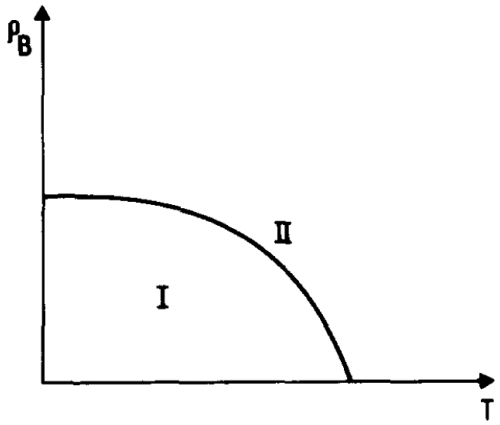

Fig. 1. Schematic phase diagram of hadronic matter. ρ_B is the density of baryonic number. Quarks are confined in phase I and unconfined in phase II.

Thermodynamics of QCD

- Gross, Wilczek (1973), Politzer (1973) – strong interactions weaken at high energies
- Cabbibo, Parisi (1975), Collins, Perry (1975) conjectured the phase structure:

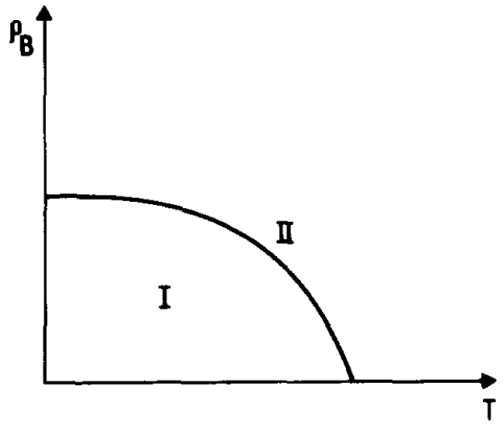

Fig. 1. Schematic phase diagram of hadronic matter. ρ_B is the density of baryonic number. Quarks are confined in phase I and unconfined in phase II.

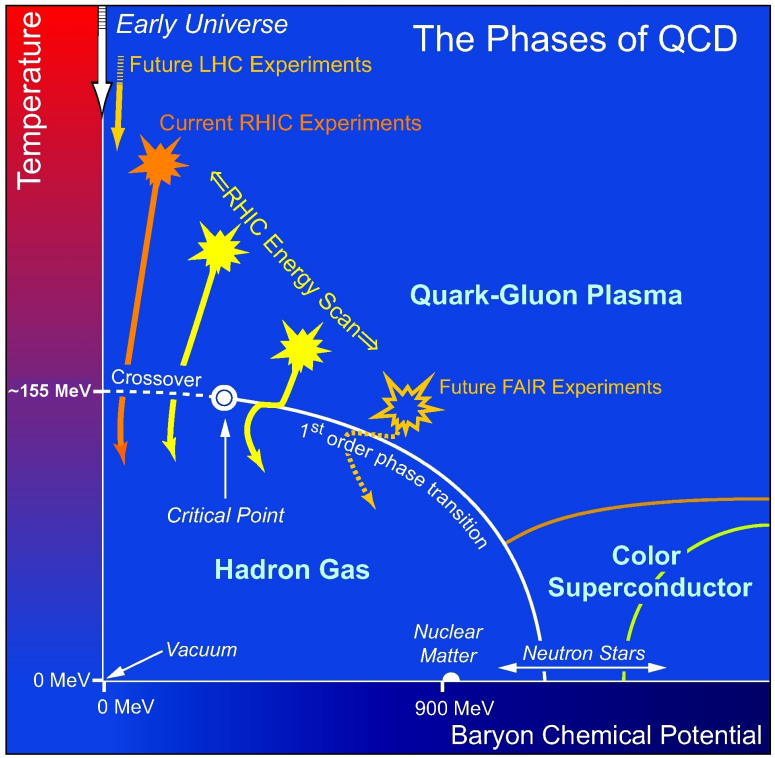

RHIC experiments

Relativistic heavy-ion collisions

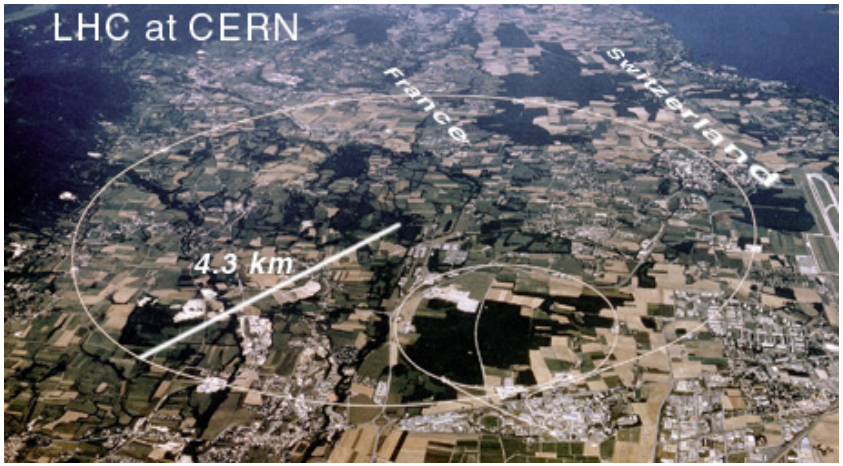

- Relativistic heavy-ion collision experiments: RHIC, BNL (Au-Au) and LHC, CERN (Pb-Pb)

Relativistic heavy-ion collisions

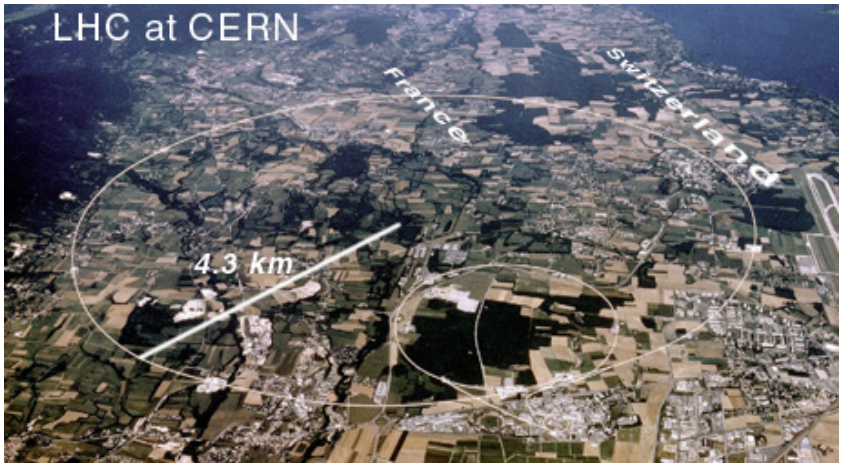

- Relativistic heavy-ion collision experiments: RHIC, BNL (Au-Au) and LHC, CERN (Pb-Pb)
- Discovery: Quark-Gluon Plasma (QGP) behaves as almost perfect fluid, rather than almost ideal gas

Relativistic heavy-ion collisions

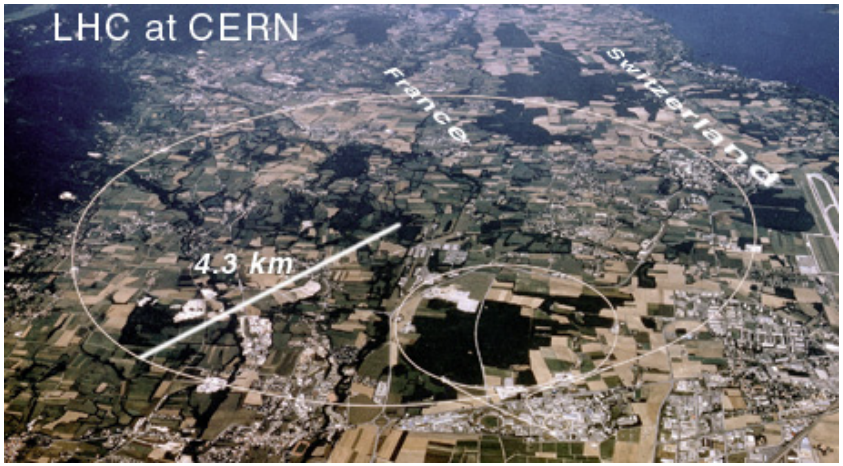

- Relativistic heavy-ion collision experiments: RHIC, BNL (Au-Au) and LHC, CERN (Pb-Pb)
- Discovery: Quark-Gluon Plasma (QGP) behaves as almost perfect fluid, rather than almost ideal gas
- Upcoming experiments: FAIR, NICA

Relativistic heavy-ion collisions

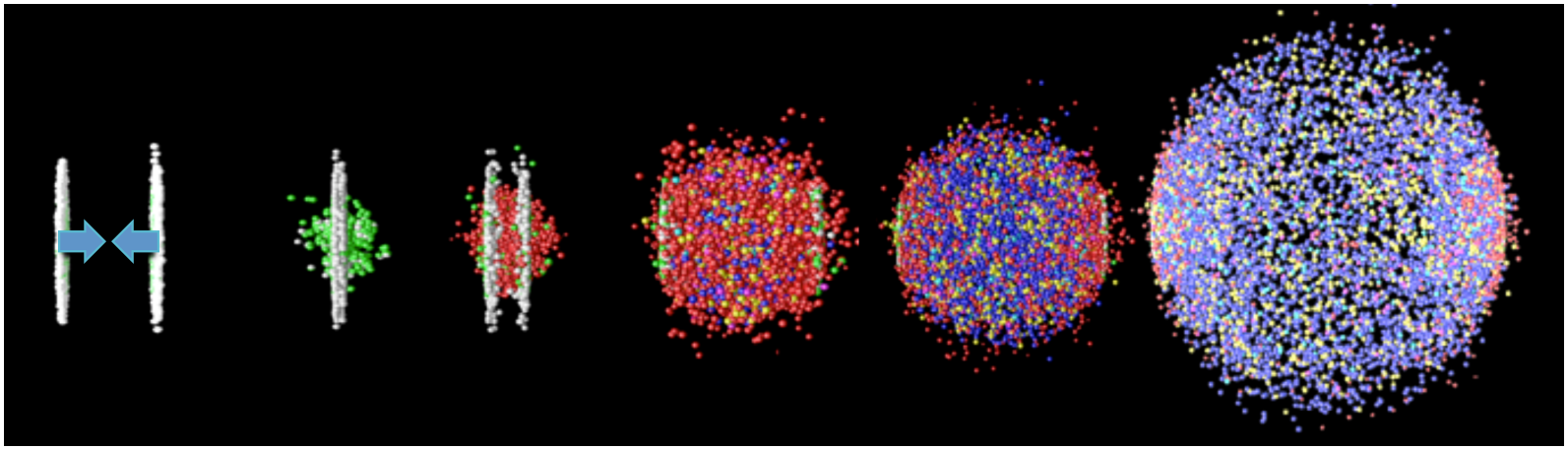

- Heavy nuclei are collided at almost the speed of light

Relativistic heavy-ion collisions

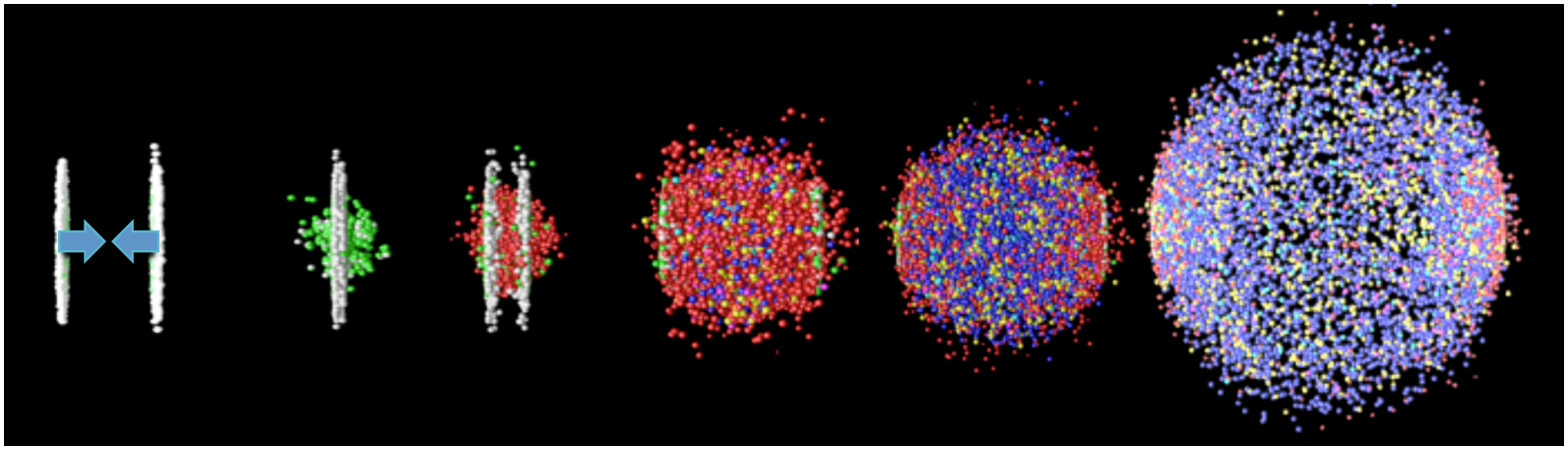

- Heavy nuclei are collided at almost the speed of light
- Hadrons melt and the Quark-Gluon Plasma is formed

Relativistic heavy-ion collisions

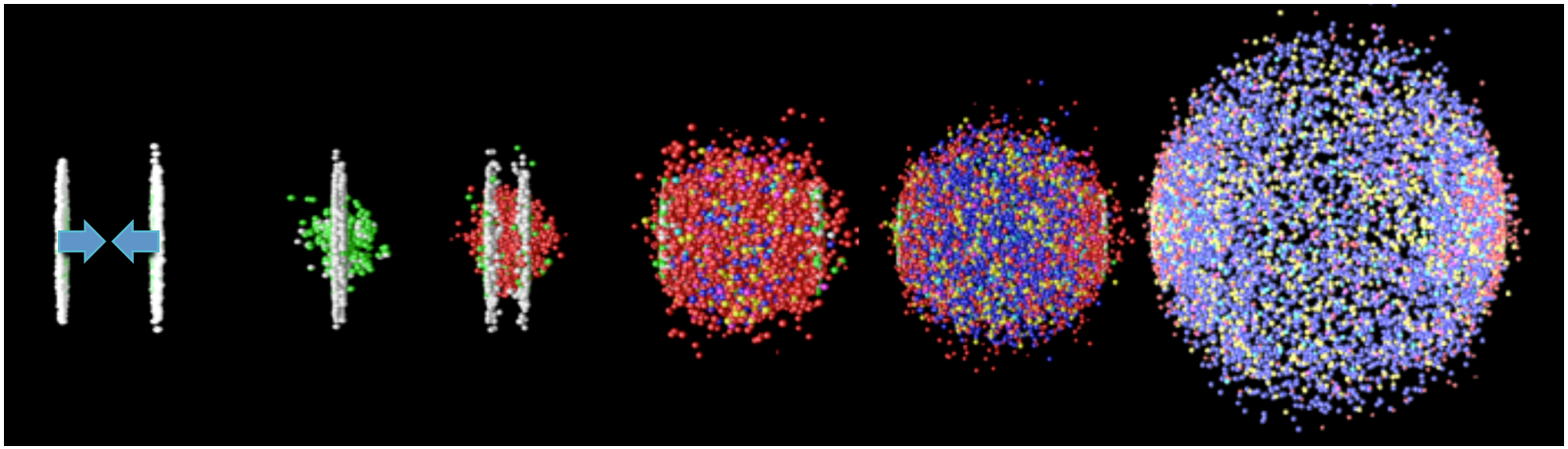

- Heavy nuclei are collided at almost the speed of light
- Hadrons melt and the Quark-Gluon Plasma is formed
- The system expands, cools and breaks down into the final state hadrons which are detected

Relativistic heavy-ion collisions

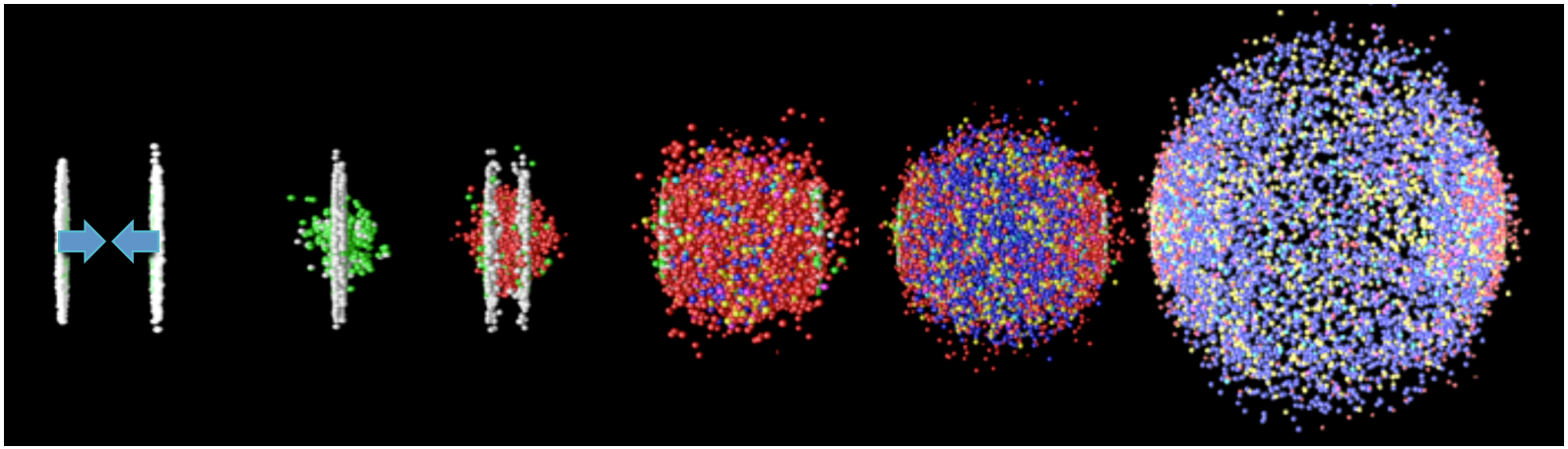

- Heavy nuclei are collided at almost the speed of light
- Hadrons melt and the Quark-Gluon Plasma is formed
- The system expands, cools and breaks down into the final state hadrons which are detected
- Chemical freeze-out: inelastic processes cease

Relativistic heavy-ion collisions

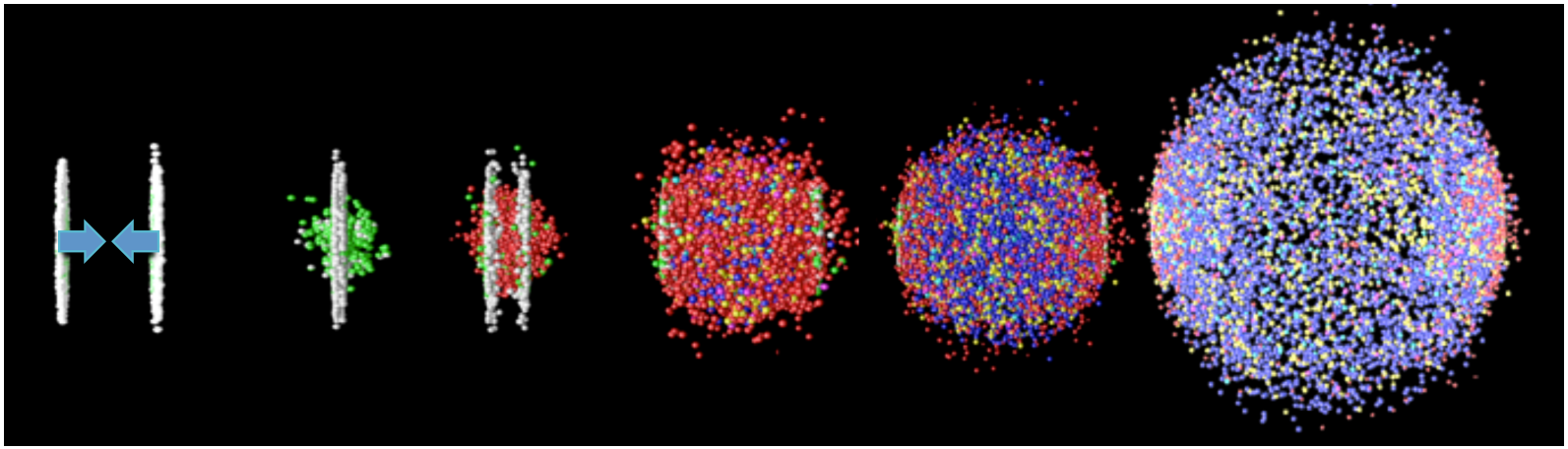

- Heavy nuclei are collided at almost the speed of light
- Hadrons melt and the Quark-Gluon Plasma is formed
- The system expands, cools and breaks down into the final state hadrons which are detected
- Chemical freeze-out: inelastic processes cease
- Kinetic freeze-out: the momenta of the particles stop changing, free streaming of hadrons

Relativistic heavy-ion collisions

- Cumulants of the event-by-event multiplicity distributions:

$$C_1 = \langle N \rangle\,,\; C_2 = \left\langle (\delta N)^2 \right\rangle,\; C_3 = \left\langle (\delta N)^3 \right\rangle,\; C_4 = \left\langle (\delta N)^4 \right\rangle - 3\left\langle (\delta N)^2 \right\rangle^2$$

Relativistic heavy-ion collisions

- Cumulants of the event-by-event multiplicity distributions:

$$C_1 = \langle N \rangle\,,\; C_2 = \left\langle (\delta N)^2 \right\rangle,\; C_3 = \left\langle (\delta N)^3 \right\rangle,\; C_4 = \left\langle (\delta N)^4 \right\rangle - 3\left\langle (\delta N)^2 \right\rangle^2$$

- Mean, variance, skewness and kurtosis:

$$M = C_1,\;\; \sigma^2 = C_2,\;\; S = \frac{C_3}{(C_2)^{\frac{3}{2}}},\;\; \kappa = \frac{C_4}{(C_2)^2}$$

Relativistic heavy-ion collisions

- Cumulants of the event-by-event multiplicity distributions:

$$C_1 = \langle N \rangle\,,\; C_2 = \left\langle (\delta N)^2 \right\rangle,\; C_3 = \left\langle (\delta N)^3 \right\rangle,\; C_4 = \left\langle (\delta N)^4 \right\rangle - 3\left\langle (\delta N)^2 \right\rangle^2$$

- Mean, variance, skewness and kurtosis:

$$M = C_1,\;\; \sigma^2 = C_2,\;\; S = \frac{C_3}{(C_2)^{\frac{3}{2}}},\;\; \kappa = \frac{C_4}{(C_2)^2}$$

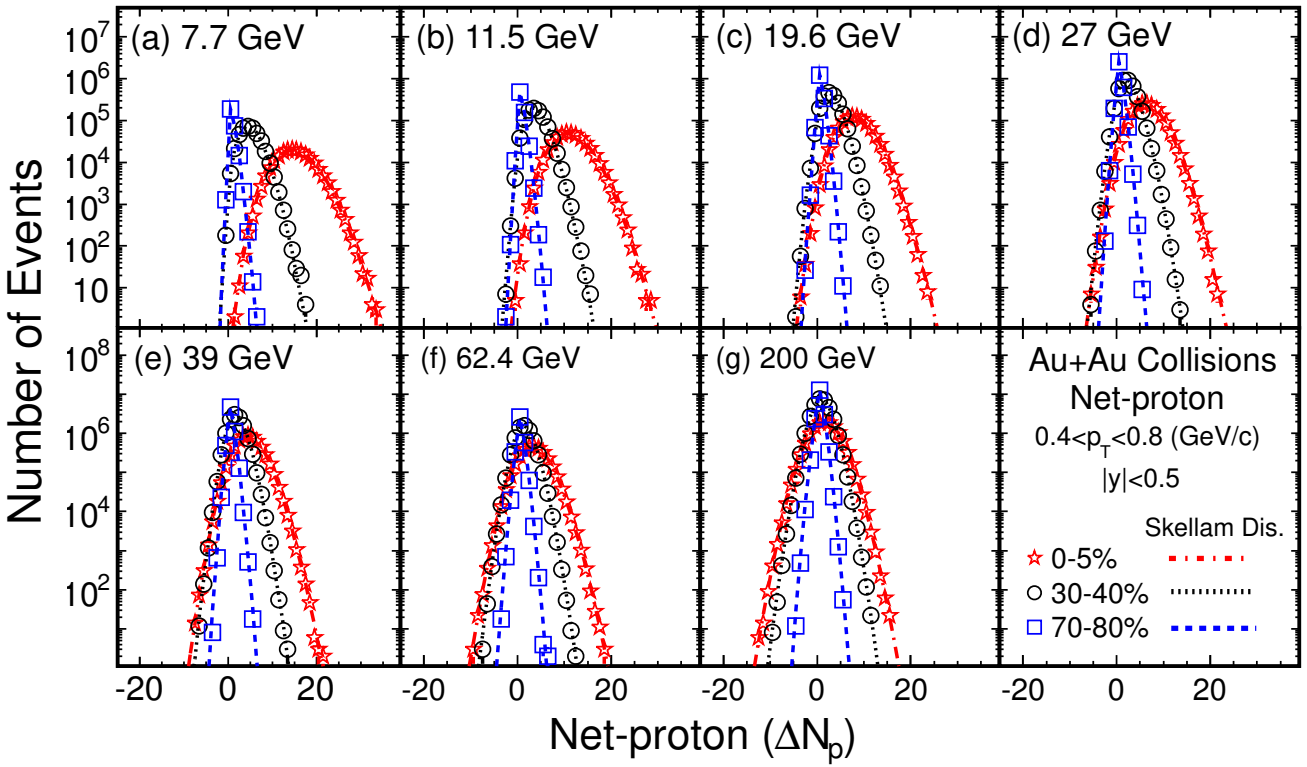

Questions to address

- What is the order of the transition to QGP at $\mu_B = 0$?
- What is the transition temperature?
- What are the signatures of deconfinement and chiral symmetry restoration?
- What is the structure of the phase diagram at $\mu_B > 0$?
- What is the equation of state of QGP?
- What happens to the QCD spectrum close to the transition?
- How do the interactions get screened in the plasma?
- When is the asymptotic regime (weakly interacting gas) is approached?

Questions to address

- What is the order of the transition to QGP at $\mu_B = 0$?
- What is the transition temperature?
- What are the signatures of deconfinement and chiral symmetry restoration?
- What is the structure of the phase diagram at $\mu_B > 0$?
- What is the equation of state of QGP?
- What happens to the QCD spectrum close to the transition?
- How do the interactions get screened in the plasma?
- When is the asymptotic regime (weakly interacting gas) is approached?

Lattice gauge theory

Strong coupling constant α_s

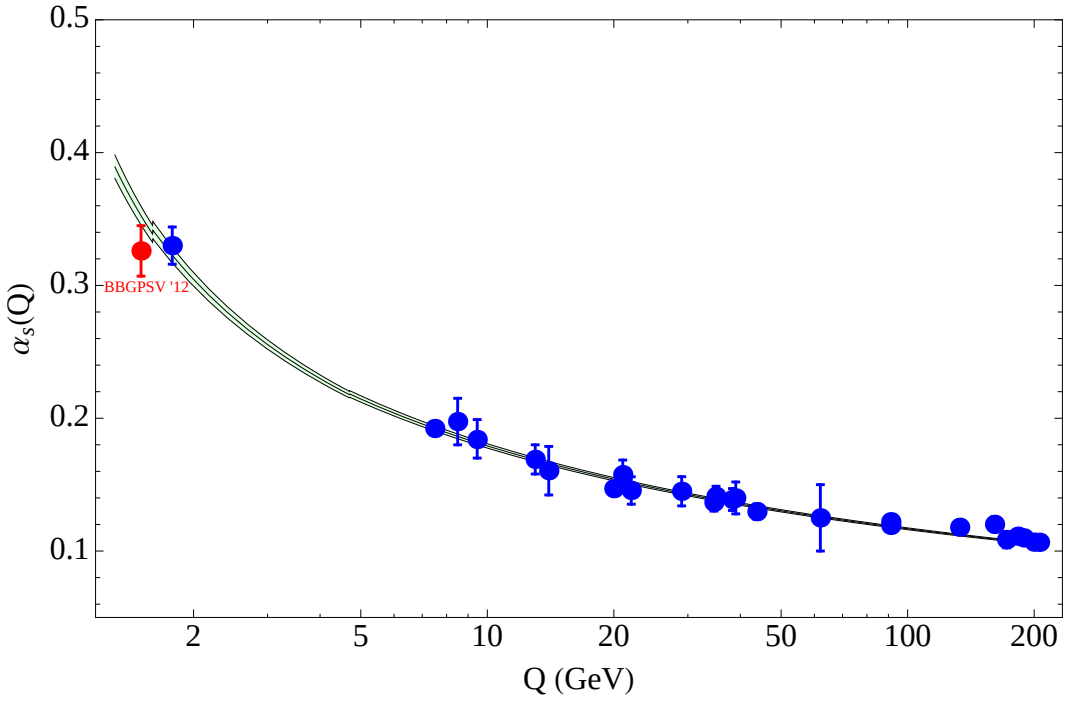

- Asymptotic freedom at high energies[1]

[1] Gross, Wilczek; Politzer (1973)
[2] Wilson (1974)

Strong coupling constant α_s

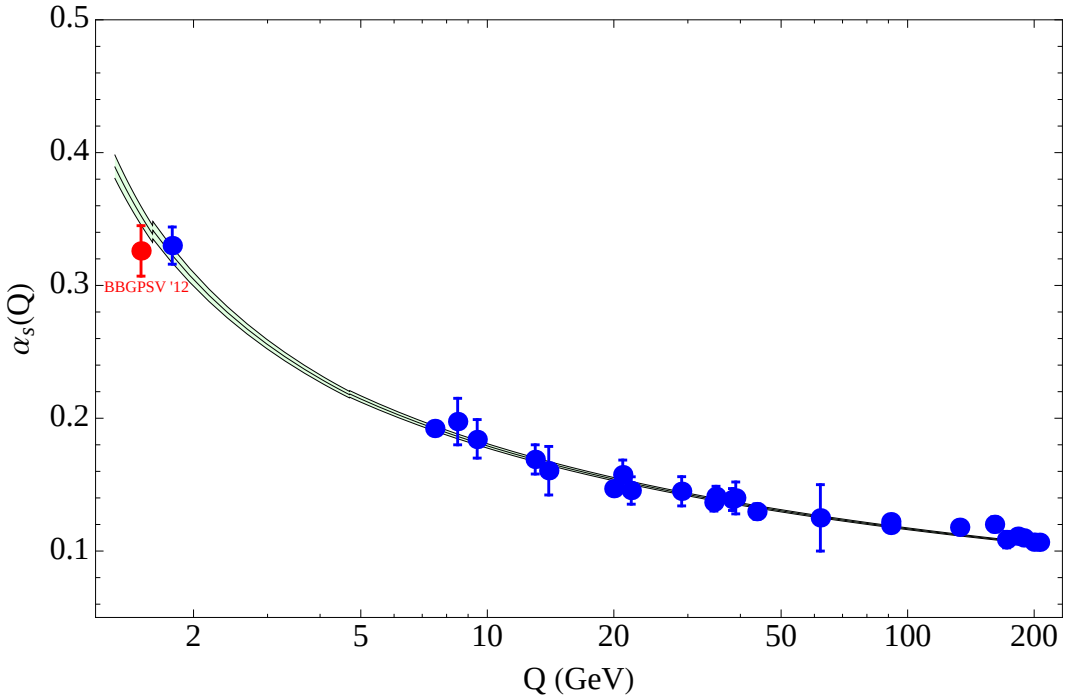

- Asymptotic freedom at high energies[1]
- Strongly coupled at low energies – Lattice QCD[2]

[1] Gross, Wilczek; Politzer (1973)
[2] Wilson (1974)

Lattice gauge theory

- Start with the path integral quantization, Euclidean signature:

$$
\begin{aligned}
\langle \mathcal{O} \rangle &= \frac{1}{\mathcal{Z}} \int \mathcal{D}[\psi]\mathcal{D}[\bar{\psi}]\mathcal{D}[A]\ \mathcal{O} \exp(-\mathcal{S}_E(T, V, \vec{\mu})), \\
\mathcal{Z}(T, V, \vec{\mu}) &= \int \mathcal{D}[\psi]\mathcal{D}[\bar{\psi}]\mathcal{D}[A] \exp(-\mathcal{S}_E(T, V, \vec{\mu})), \\
\mathcal{S}_E(T, V, \vec{\mu}) &= -\int_0^{1/T} dx_0 \int_V d^3\mathbf{x} \mathcal{L}^E(\vec{\mu}), \\
\mathcal{L}^E(\vec{\mu}) &= \mathcal{L}^E_{QCD} + \sum_{f=u,d,s} \mu_f \bar{\psi}_f \gamma_0 \psi_f
\end{aligned}
$$

Lattice gauge theory

- Start with the path integral quantization, Euclidean signature:

$$
\begin{aligned}
\langle \mathcal{O} \rangle &= \frac{1}{\mathcal{Z}} \int \mathcal{D}[\psi]\mathcal{D}[\bar{\psi}]\mathcal{D}[A]\ \mathcal{O} \exp(-\mathcal{S}_E(T, V, \vec{\mu})), \\
\mathcal{Z}(T, V, \vec{\mu}) &= \int \mathcal{D}[\psi]\mathcal{D}[\bar{\psi}]\mathcal{D}[A] \exp(-\mathcal{S}_E(T, V, \vec{\mu})), \\
\mathcal{S}_E(T, V, \vec{\mu}) &= -\int_0^{1/T} dx_0 \int_V d^3\mathbf{x} \mathcal{L}^E(\vec{\mu}), \\
\mathcal{L}^E(\vec{\mu}) &= \mathcal{L}^E_{QCD} + \sum_{f=u,d,s} \mu_f \bar{\psi}_f \gamma_0 \psi_f
\end{aligned}
$$

- Introduce a (non-perturbative!) regulator – minimum space-time "resolution" scale a, i.e. lattice, Wilson (1974)

Lattice gauge theory

- Start with the path integral quantization, Euclidean signature:

$$
\begin{aligned}
\langle \mathcal{O} \rangle &= \frac{1}{\mathcal{Z}} \int \mathcal{D}[\psi]\mathcal{D}[\bar{\psi}]\mathcal{D}[A]\ \mathcal{O} \exp(-\mathcal{S}_E(T, V, \vec{\mu})), \\
\mathcal{Z}(T, V, \vec{\mu}) &= \int \mathcal{D}[\psi]\mathcal{D}[\bar{\psi}]\mathcal{D}[A] \exp(-\mathcal{S}_E(T, V, \vec{\mu})), \\
\mathcal{S}_E(T, V, \vec{\mu}) &= -\int_0^{1/T} dx_0 \int_V d^3\mathbf{x} \mathcal{L}^E(\vec{\mu}), \\
\mathcal{L}^E(\vec{\mu}) &= \mathcal{L}^E_{QCD} + \sum_{f=u,d,s} \mu_f \bar{\psi}_f \gamma_0 \psi_f
\end{aligned}
$$

- Introduce a (non-perturbative!) regulator – minimum space-time "resolution" scale a, i.e. lattice, Wilson (1974)
- The lattice spacing a acts as a UV cutoff, $p_{max} \sim \pi/a$

Lattice gauge theory

- Start with the path integral quantization, Euclidean signature:

$$
\begin{aligned}
\langle \mathcal{O} \rangle &= \frac{1}{\mathcal{Z}} \int \mathcal{D}[\psi]\mathcal{D}[\bar{\psi}]\mathcal{D}[A]\ \mathcal{O} \exp(-\mathcal{S}_E(T, V, \vec{\mu})), \\
\mathcal{Z}(T, V, \vec{\mu}) &= \int \mathcal{D}[\psi]\mathcal{D}[\bar{\psi}]\mathcal{D}[A] \exp(-\mathcal{S}_E(T, V, \vec{\mu})), \\
\mathcal{S}_E(T, V, \vec{\mu}) &= -\int_0^{1/T} dx_0 \int_V d^3\mathbf{x} \mathcal{L}^E(\vec{\mu}), \\
\mathcal{L}^E(\vec{\mu}) &= \mathcal{L}^E_{QCD} + \sum_{f=u,d,s} \mu_f \bar{\psi}_f \gamma_0 \psi_f
\end{aligned}
$$

- Introduce a (non-perturbative!) regulator – minimum space-time "resolution" scale a, i.e. lattice, Wilson (1974)
- The lattice spacing a acts as a UV cutoff, $p_{max} \sim \pi/a$
- The integrals can be evaluated with importance sampling methods

Challenges

- Broken symmetries – e.g., Lorentz, chiral

Challenges

- Broken symmetries – e.g., Lorentz, chiral
- Grassmann fields (fermions) cannot be sampled, integrate them out:

$$
\begin{aligned}
Z &= \int \mathcal{D}[U]\mathcal{D}[\psi]\mathcal{D}[\bar{\psi}]e^{-\mathcal{S}_G[U]-\mathcal{S}_F[\bar{\psi},\psi,U]} \\
&= \int \mathcal{D}[U]e^{-\mathcal{S}_G[U]} \det|M[U]|
\end{aligned}
$$

Challenges

- Broken symmetries – e.g., Lorentz, chiral
- Grassmann fields (fermions) cannot be sampled, integrate them out:

$$
\begin{aligned}
Z &= \int \mathcal{D}[U]\mathcal{D}[\psi]\mathcal{D}[\bar{\psi}]e^{-\mathcal{S}_G[U]-\mathcal{S}_F[\bar{\psi},\psi,U]} \\
&= \int \mathcal{D}[U]e^{-\mathcal{S}_G[U]} \det|M[U]|
\end{aligned}
$$

- The effective action is highly non-local, Monte Carlo sampling is costly
- The computational cost is determined by the condition number of the fermion matrix, which scales with the inverse lightest quark mass

Challenges

- Broken symmetries – e.g., Lorentz, chiral
- Grassmann fields (fermions) cannot be sampled, integrate them out:

$$
\begin{aligned}
Z &= \int \mathcal{D}[U]\mathcal{D}[\psi]\mathcal{D}[\bar{\psi}]e^{-\mathcal{S}_G[U]-\mathcal{S}_F[\bar{\psi},\psi,U]} \\
&= \int \mathcal{D}[U]e^{-\mathcal{S}_G[U]} \det|M[U]|
\end{aligned}
$$

- The effective action is highly non-local, Monte Carlo sampling is costly
- The computational cost is determined by the condition number of the fermion matrix, which scales with the inverse lightest quark mass
- Sign problem at $\mu_B > 0$

Challenges

- Broken symmetries – e.g., Lorentz, chiral
- Grassmann fields (fermions) cannot be sampled, integrate them out:

$$
\begin{aligned}
Z &= \int \mathcal{D}[U]\mathcal{D}[\psi]\mathcal{D}[\bar{\psi}]e^{-\mathcal{S}_G[U]-\mathcal{S}_F[\bar{\psi},\psi,U]} \\
&= \int \mathcal{D}[U]e^{-\mathcal{S}_G[U]} \det|M[U]|
\end{aligned}
$$

- The effective action is highly non-local, Monte Carlo sampling is costly
- The computational cost is determined by the condition number of the fermion matrix, which scales with the inverse lightest quark mass
- Sign problem at $\mu_B > 0$
- Real-time properties are hard to access

Results at $\mu_B = 0$

Early lattice results

First study of the deconfinement transition in $SU(2)$ pure gauge theory:

- McLerran, Svetitsky (1981) $T_c = 200$ MeV, Polyakov loop (left)
- Kuti et al. (1981) $T_c = 160 \pm 30$ MeV,
- Engels et al. (1981) $T_c = 210 \pm 10$ MeV, energy density (right)

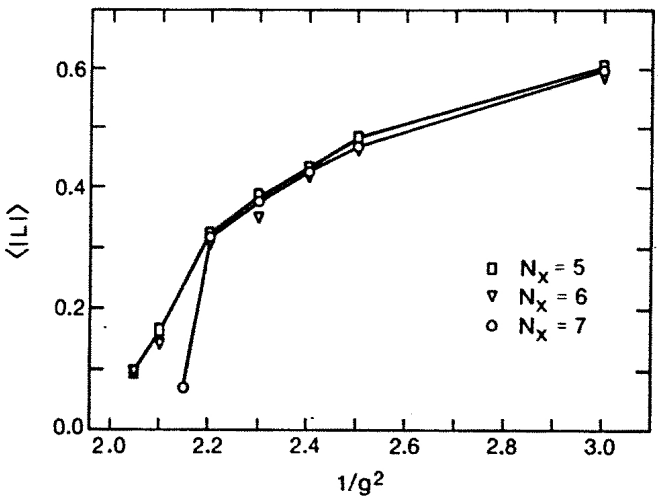

Fig. 2. Magnetization curves for $N_t = 3$. We display $\langle |L| \rangle$ rather than $\langle L \rangle$ to remove effects of domain nucleation as shown in fig. 1. Points for $N_x = 5$ and for $N_x = 7$ are joined to guide the eye.

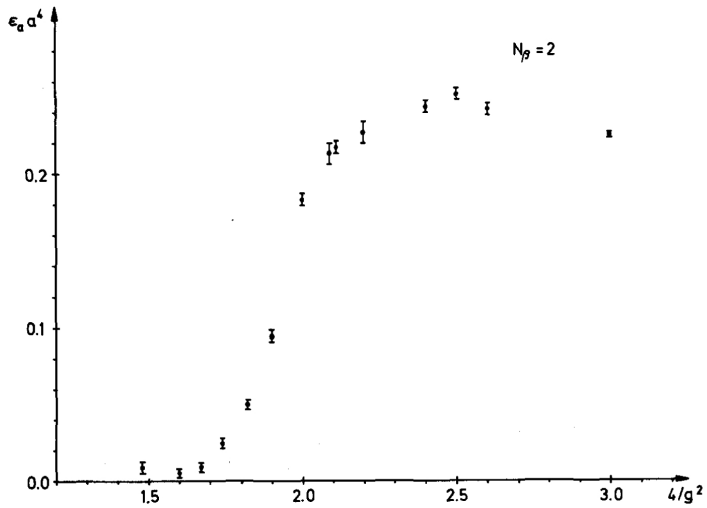

Fig. 3. Energy density of gluon matter versus $4/g^2$, at fixed lattice size $N_\beta = 2$, after about 500 iterations.

Chiral symmetry restoration

$$\langle\bar{\psi}\psi\rangle_f = \frac{T}{V}\frac{\partial \ln \mathcal{Z}}{\partial m_f}, \quad \chi(T) = \frac{\partial\langle\bar{\psi}\psi\rangle_f}{\partial m_f}$$

Chiral symmetry restoration

$$\langle\bar{\psi}\psi\rangle_f = \frac{T}{V}\frac{\partial \ln \mathcal{Z}}{\partial m_f}, \quad \chi(T) = \frac{\partial\langle\bar{\psi}\psi\rangle_f}{\partial m_f}$$

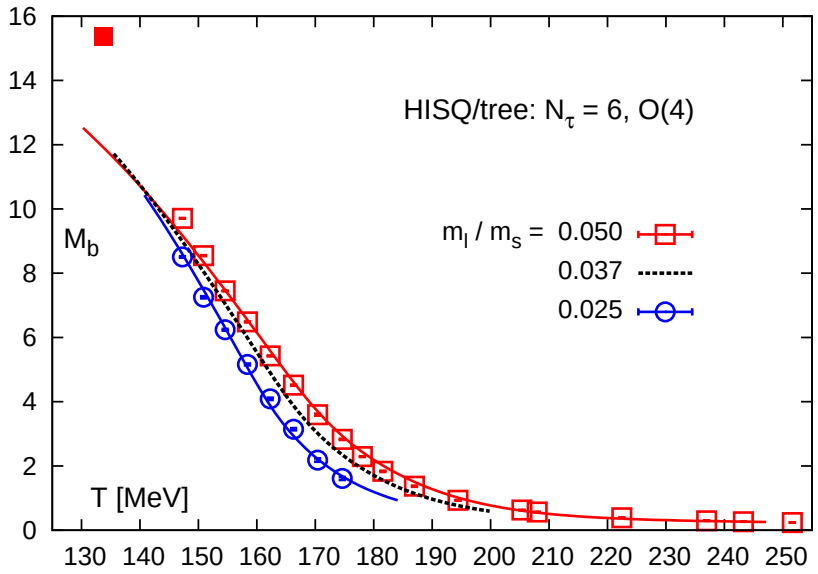

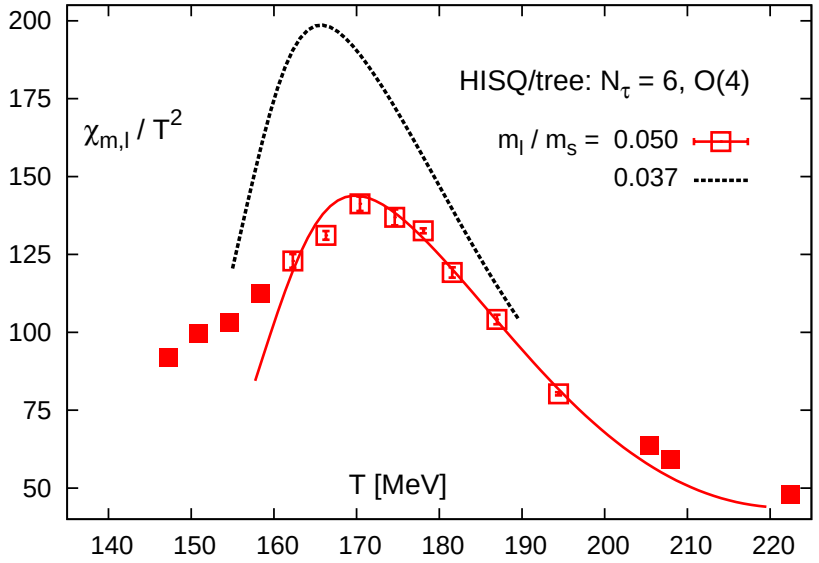

Chiral symmetry restoration

$$\langle\bar{\psi}\psi\rangle_f = \frac{T}{V}\frac{\partial \ln \mathcal{Z}}{\partial m_f}, \quad \chi(T) = \frac{\partial\langle\bar{\psi}\psi\rangle_f}{\partial m_f}$$

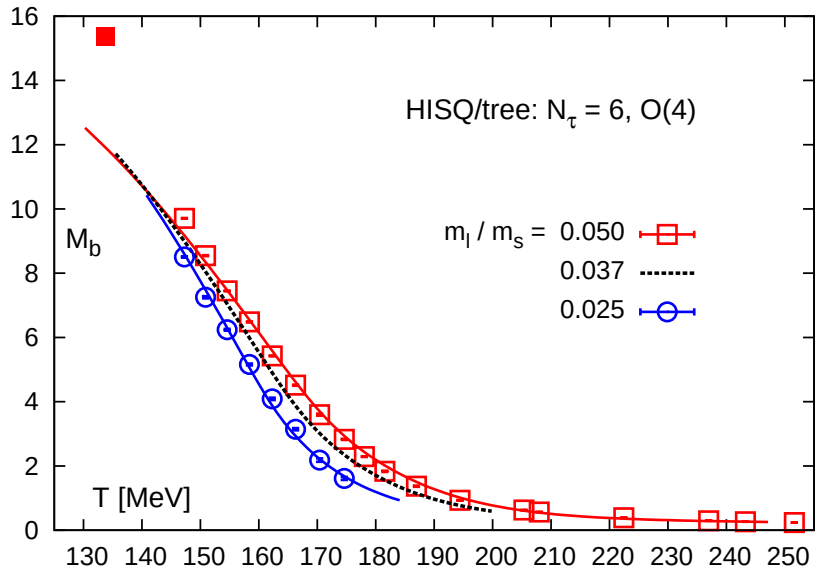

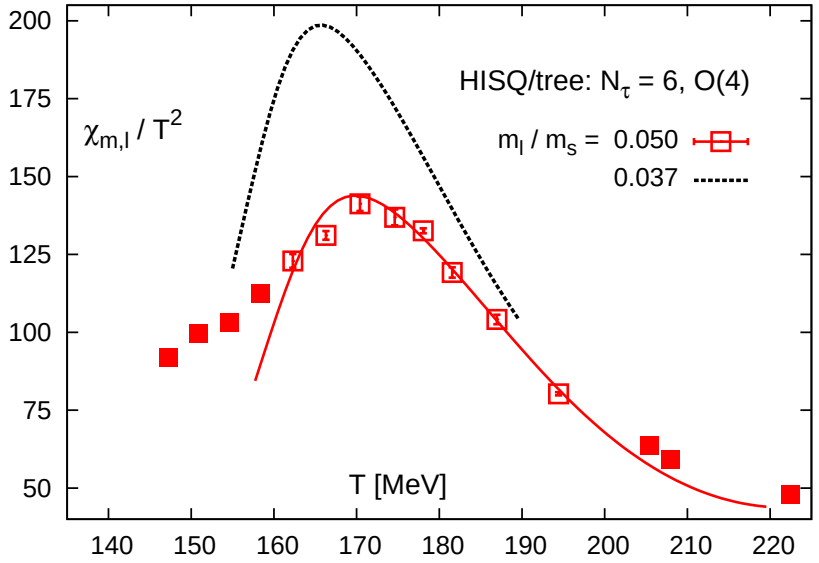

The chiral crossover temperature at $\mu_B = 0$ (Borsanyi et al. [BW] (2010), Bazavov et al. [HotQCD] (2012))

$$T_c = 154 \pm 9 \text{ MeV}$$

Curvature of the chiral crossover line

- Change in the chiral crossover temperature with μ_B

$$T_c(\mu_B) = T_c(0)\left(1 - \kappa_2\left(\frac{\mu_B}{T_c(0)}\right)^2\right)$$

Curvature of the chiral crossover line

- Change in the chiral crossover temperature with μ_B

$$T_c(\mu_B) = T_c(0)\left(1 - \kappa_2\left(\frac{\mu_B}{T_c(0)}\right)^2\right)$$

- The curvature has been estimated:
  - $\kappa_2 = 0.0066(7)$, Kaczmarek et al. (2011), Endrodi et al. (2011)
  - $\kappa_2 = 0.0135(20)$, Bonati et al. (2015)
  - $\kappa_2 = 0.0149(21)$, Belweid et al. (2015)
  - $\kappa_2 = 0.020(4)$, Cea et al. (2016)
- See talk by F. Negro today

Deconfinement

- The chemical potentials for conserved charges B, Q, S:

$$\begin{aligned}
\mu_u &= \frac{1}{3}\mu_B + \frac{2}{3}\mu_Q, \\
\mu_d &= \frac{1}{3}\mu_B - \frac{1}{3}\mu_Q, \\
\mu_s &= \frac{1}{3}\mu_B - \frac{1}{3}\mu_Q - \mu_S
\end{aligned}$$

Deconfinement

- The chemical potentials for conserved charges B, Q, S:

$$\begin{aligned}
\mu_u &= \frac{1}{3}\mu_B + \frac{2}{3}\mu_Q, \\
\mu_d &= \frac{1}{3}\mu_B - \frac{1}{3}\mu_Q, \\
\mu_s &= \frac{1}{3}\mu_B - \frac{1}{3}\mu_Q - \mu_S
\end{aligned}$$

- The pressure can be expanded in Taylor series

$$\frac{P}{T^4} = \frac{1}{VT^3} \ln \mathcal{Z}(T, V, \hat{\mu}_u, \hat{\mu}_d, \hat{\mu}_s) = \sum_{i,j,k=0}^{\infty} \frac{\chi_{ijk}^{BQS}}{i!j!\,k!} \hat{\mu}_B^i \hat{\mu}_Q^j \hat{\mu}_S^k$$

Deconfinement

- The chemical potentials for conserved charges B, Q, S:

$$\begin{aligned}\mu_u &= \frac{1}{3}\mu_B + \frac{2}{3}\mu_Q,\\ \mu_d &= \frac{1}{3}\mu_B - \frac{1}{3}\mu_Q,\\ \mu_s &= \frac{1}{3}\mu_B - \frac{1}{3}\mu_Q - \mu_S\end{aligned}$$

- The pressure can be expanded in Taylor series

$$\frac{P}{T^4} = \frac{1}{VT^3}\ln \mathcal{Z}(T, V, \hat{\mu}_u, \hat{\mu}_d, \hat{\mu}_s) = \sum_{i,j,k=0}^{\infty} \frac{\chi_{ijk}^{BQS}}{i!j!\,k!}\hat{\mu}_B^i \hat{\mu}_Q^j \hat{\mu}_S^k$$

- The generalized susceptibilities are evaluated at vanishing chemical potential

$$\chi_{ijk}^{BQS} \equiv \chi_{ijk}^{BQS}(T) = \left.\frac{\partial P(T,\hat{\mu})/T^4}{\partial\hat{\mu}_B^i \partial\hat{\mu}_Q^j \partial\hat{\mu}_S^k}\right|_{\hat{\mu}=0}, \quad \hat{\mu} \equiv \frac{\mu}{T}$$

Deconfinement: fluctuations

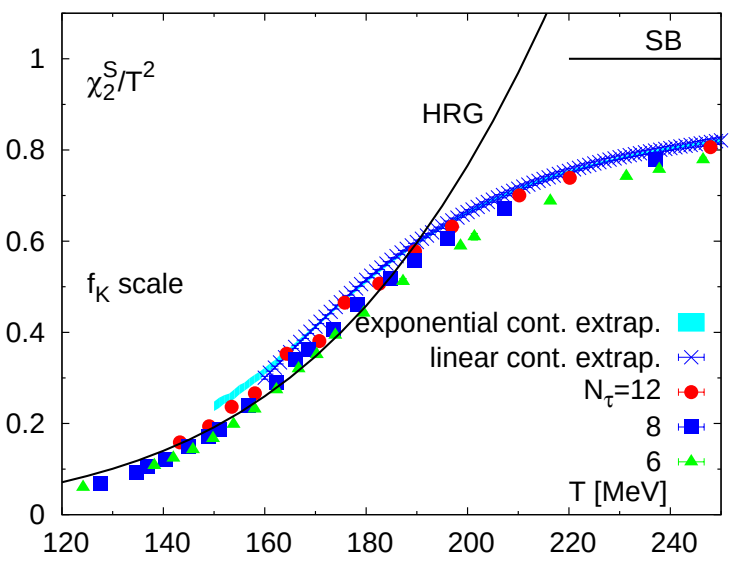

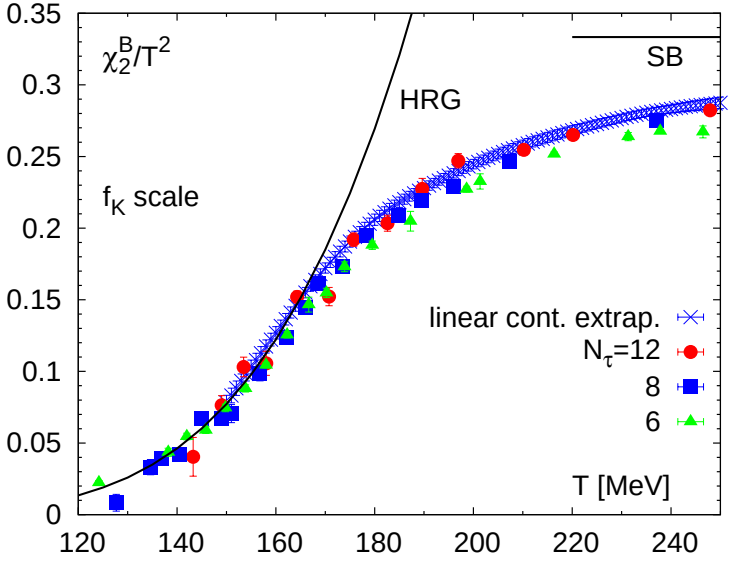

- Strangeness (left) and baryon number (right) fluctuations[3]
- Up to $\sim$ 150 MeV fluctuations can be described in terms of hadronic degrees of freedom

[3] Bazavov et al. [HotQCD] (2012)

Deconfinement: equation of state

- The equation of state has been recently calculated in the continuum limit at the physical quark masses (Borsanyi et al. [BW] (2014), Bazavov et al. [HotQCD] (2014))

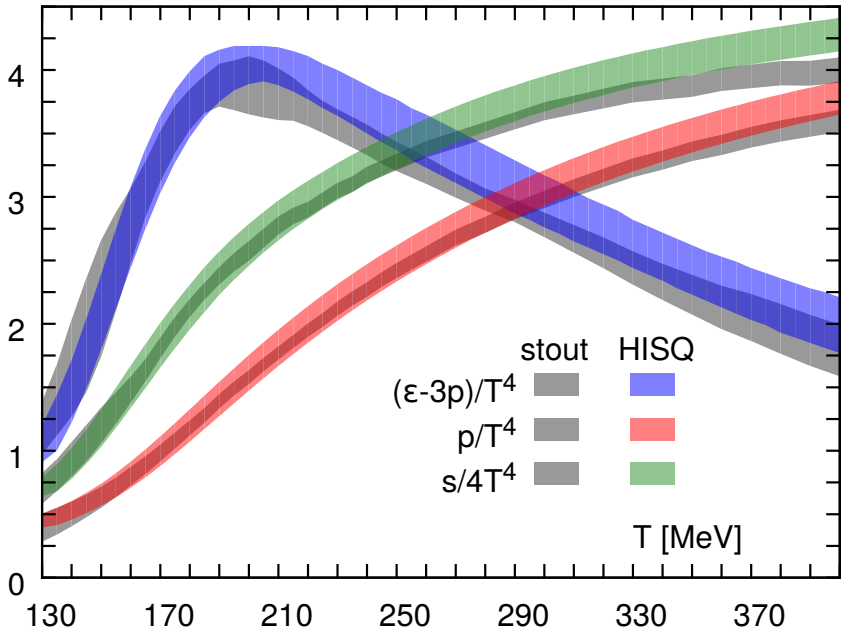

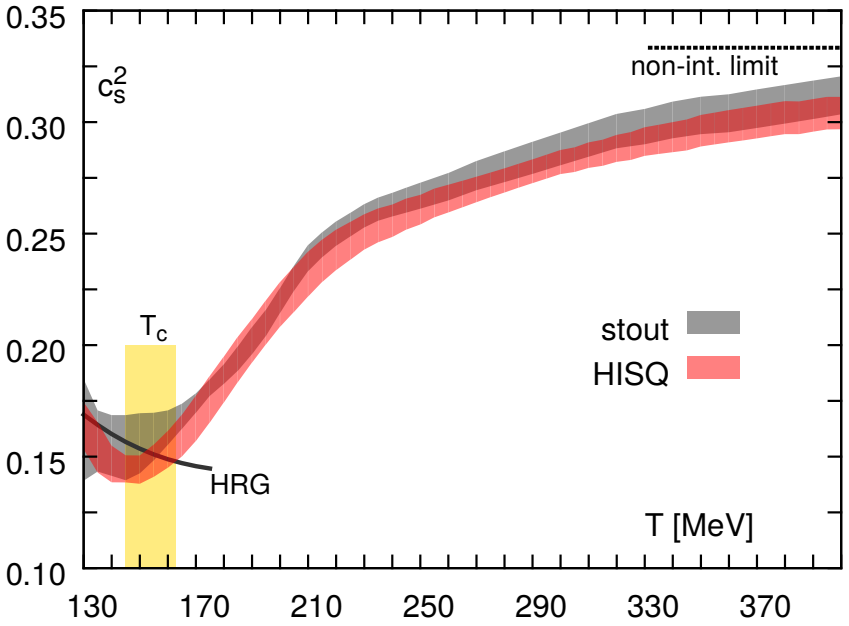

Results at $\mu_B > 0$

How to access $\mu_B > 0$?

- Direct Monte Carlo simulations are not possible due to the sign problem

How to access $\mu_B > 0$?

- Direct Monte Carlo simulations are not possible due to the sign problem
- **Method 1**: Taylor expansion (Allton et al. (2002)), evaluate various derivatives at $\mu = 0$, e.g.

$$\chi_2^u = \frac{T}{V}\left\langle \mathrm{Tr}\left(M_u^{-1}M_u'' - (M_u^{-1}M_u')^2\right) + \left(\mathrm{Tr}(M_u^{-1}M_u')\right)^2\right\rangle$$

How to access $\mu_B > 0$?

- Direct Monte Carlo simulations are not possible due to the sign problem
- **Method 1**: Taylor expansion (Allton et al. (2002)), evaluate various derivatives at $\mu = 0$, e.g.

$$\chi_2^u = \frac{T}{V}\left\langle \mathrm{Tr}\left(M_u^{-1}M_u'' - (M_u^{-1}M_u')^2\right) + \left(\mathrm{Tr}(M_u^{-1}M_u')\right)^2\right\rangle$$

- **Method 2**: Perform simulations at imaginary chemical potential, then evaluate the derivatives of $P(i\mu)$ (Lombardo (1999), de Forcrand, Philipsen (2002))

Constrained series expansions

- The number densities can also be represented with Taylor expansions:

$$\frac{n_X}{T^3} = \frac{\partial P/T^4}{\partial \hat{\mu}_X}, \;\; X = B, Q, S$$

Constrained series expansions

- The number densities can also be represented with Taylor expansions:

$$\frac{n_X}{T^3} = \frac{\partial P/T^4}{\partial \hat{\mu}_X}, \;\; X = B, Q, S$$

- In heavy-ion collisions there are additional constraints:

$$n_S = 0, \;\; \frac{n_Q}{n_B} = 0.4$$

Constrained series expansions

- The number densities can also be represented with Taylor expansions:

$$\frac{n_X}{T^3} = \frac{\partial P/T^4}{\partial \hat{\mu}_X}, \;\; X = B, Q, S$$

- In heavy-ion collisions there are additional constraints:

$$n_S = 0, \;\; \frac{n_Q}{n_B} = 0.4$$

- These constraints can be fulfilled by

$$\begin{aligned} \hat{\mu}_Q(T, \mu_B) &= q_1(T)\hat{\mu}_B + q_3(T)\hat{\mu}_B^3 + q_5(T)\hat{\mu}_B^5 + \dots \,, \\ \hat{\mu}_S(T, \mu_B) &= s_1(T)\hat{\mu}_B + s_3(T)\hat{\mu}_B^3 + s_5(T)\hat{\mu}_B^5 + \dots \end{aligned}$$

Freeze-out parameters

- Consider the ratios of cumulants:

$$R_{31}^{Q} = \frac{S_Q \sigma_Q^3}{M_Q} = \frac{\chi_3^Q}{\chi_1^Q}, \quad R_{12}^{Q} = \frac{M_Q}{\sigma_Q^2} = \frac{\chi_1^Q}{\chi_2^Q}$$

Freeze-out parameters

- Consider the ratios of cumulants:

$$R_{31}^{Q} = \frac{S_Q \sigma_Q^3}{M_Q} = \frac{\chi_3^Q}{\chi_1^Q}, \quad R_{12}^{Q} = \frac{M_Q}{\sigma_Q^2} = \frac{\chi_1^Q}{\chi_2^Q}$$

- These ratios can be evaluated on the lattice for constrained system and serve as thermometer (left) and baryometer (right) (Bazavov et al. (2012))

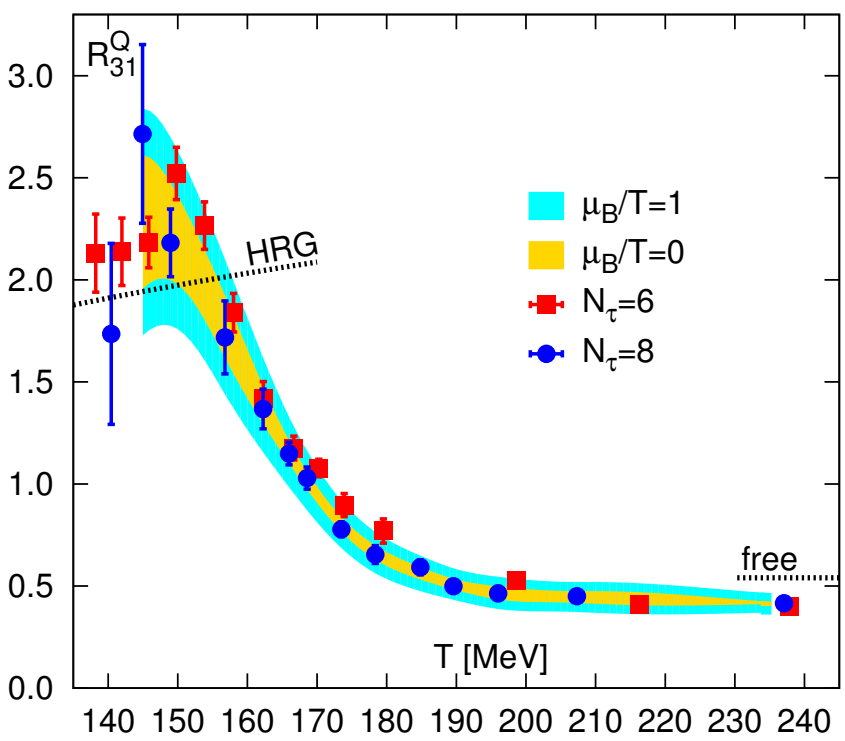

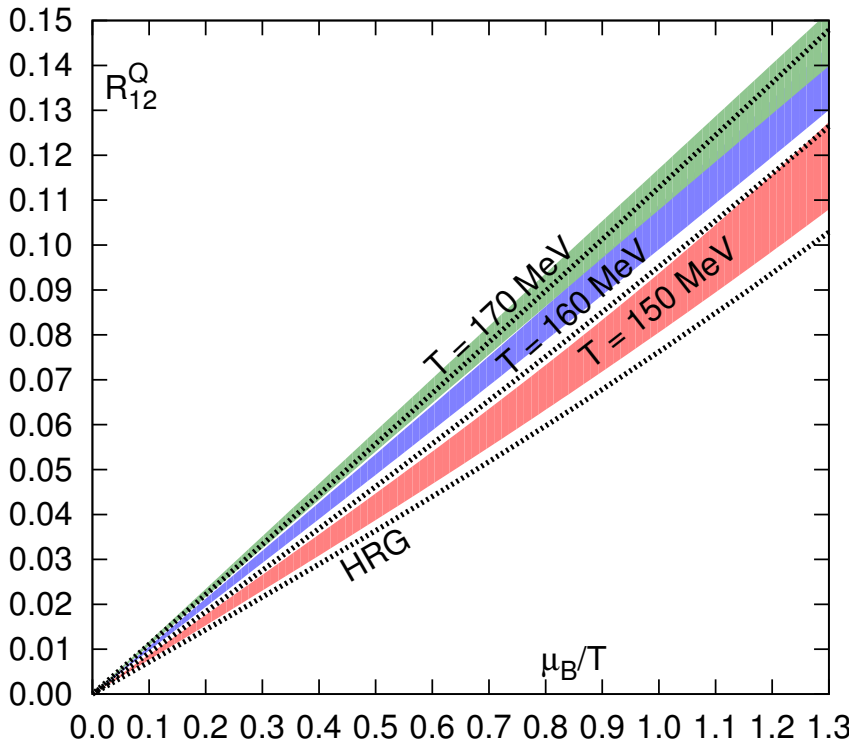

The equation of state at $O(\mu_B^6)$

- Consider $\mu_Q = \mu_S = 0$ then the pressure is given by[4]

$$\frac{\Delta P}{T^4} = \frac{1}{2}\chi_2^B(T)\hat{\mu}_B^2 \left(1 + \frac{1}{12}\frac{\chi_4^B(T)}{\chi_2^B(T)}\hat{\mu}_B^2 + \frac{1}{360}\frac{\chi_6^B(T)}{\chi_2^B(T)}\hat{\mu}_B^4 + \ ...\right)$$

[4] Bazavov et al. [HotQCD] (2017)

The equation of state at $O(\mu_B^6)$

- Consider $\mu_Q = \mu_S = 0$ then the pressure is given by[4]

$$\frac{\Delta P}{T^4} = \frac{1}{2}\chi_2^B(T)\hat{\mu}_B^2\left(1 + \frac{1}{12}\frac{\chi_4^B(T)}{\chi_2^B(T)}\hat{\mu}_B^2 + \frac{1}{360}\frac{\chi_6^B(T)}{\chi_2^B(T)}\hat{\mu}_B^4 + \ \ldots\right)$$

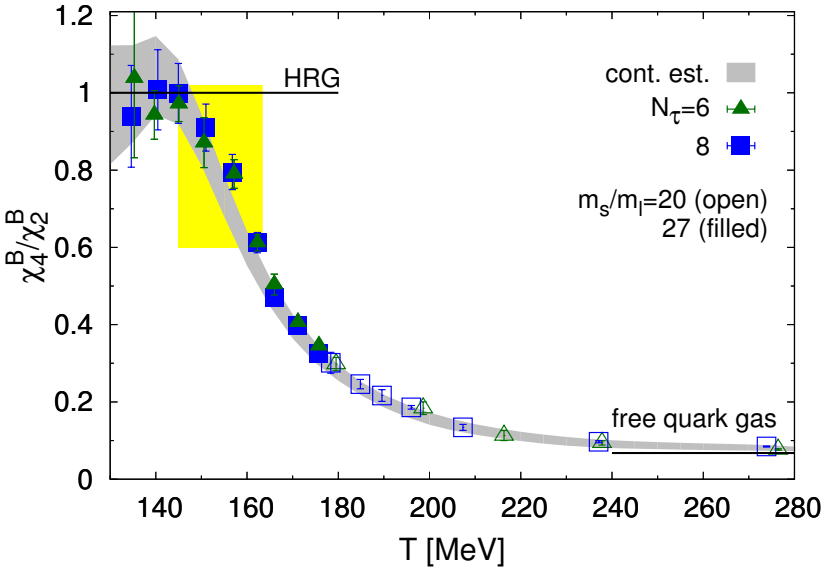

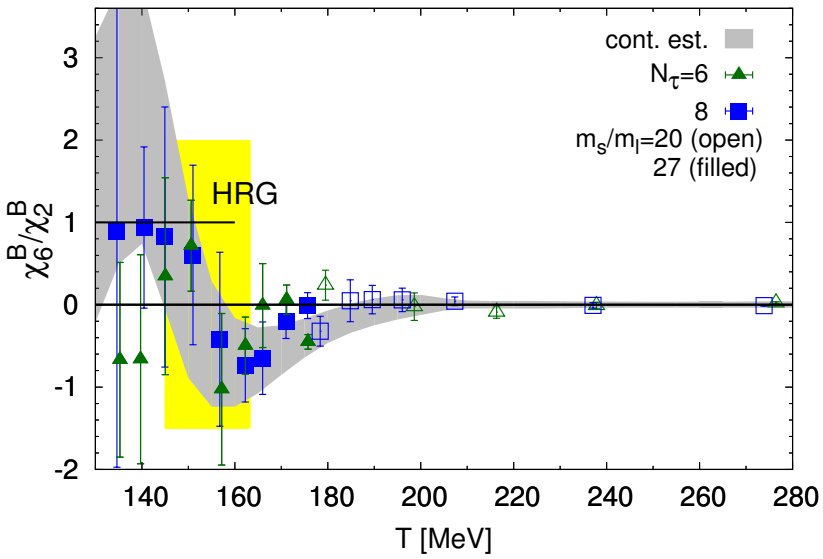

[4] Bazavov et al. [HotQCD] (2017)

The equation of state at $O(\mu_B^6)$

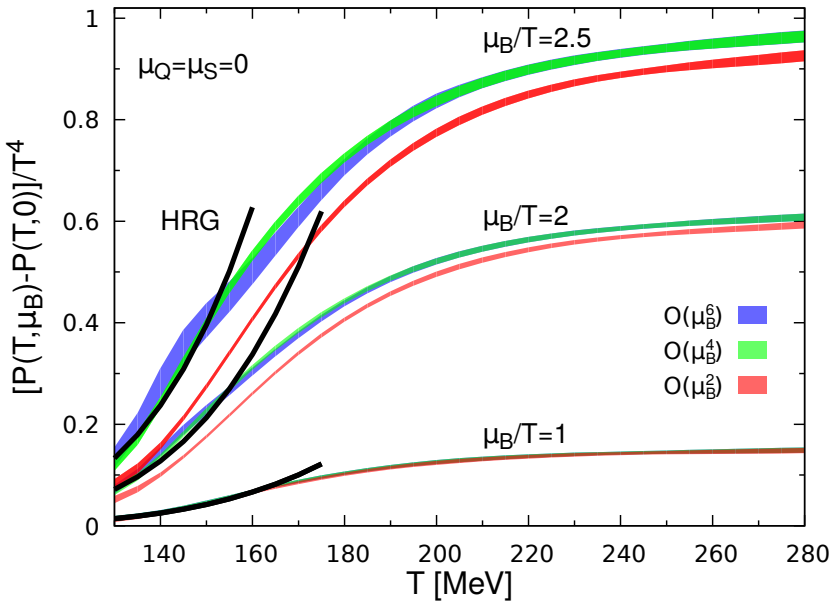

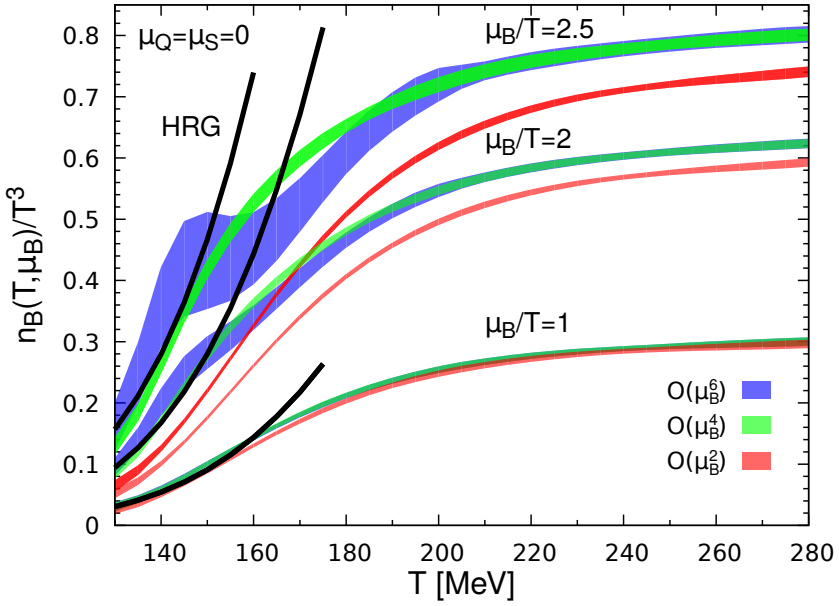

- The contribution to the pressure due to finite chemical potential (left) and the baryon number density (right)

The equation of state at $O(\mu_B^6)$

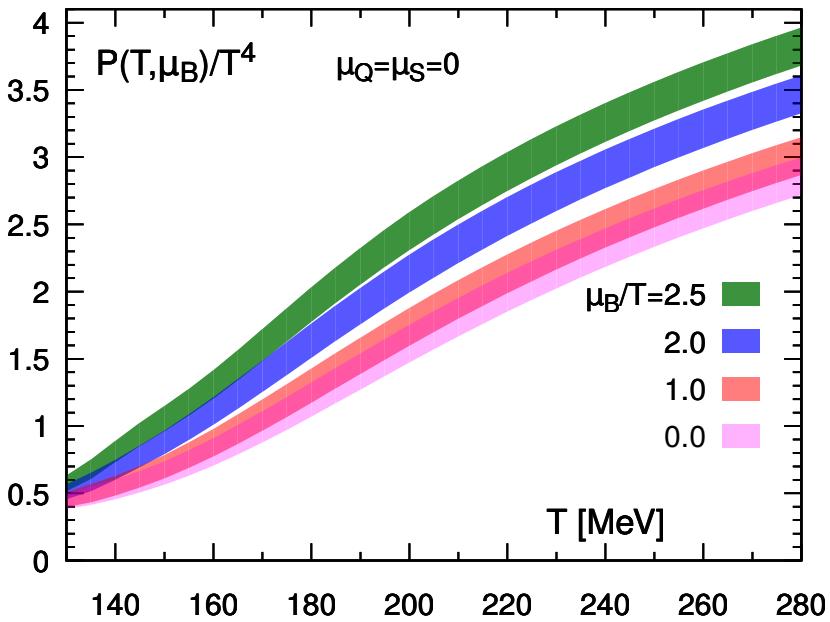

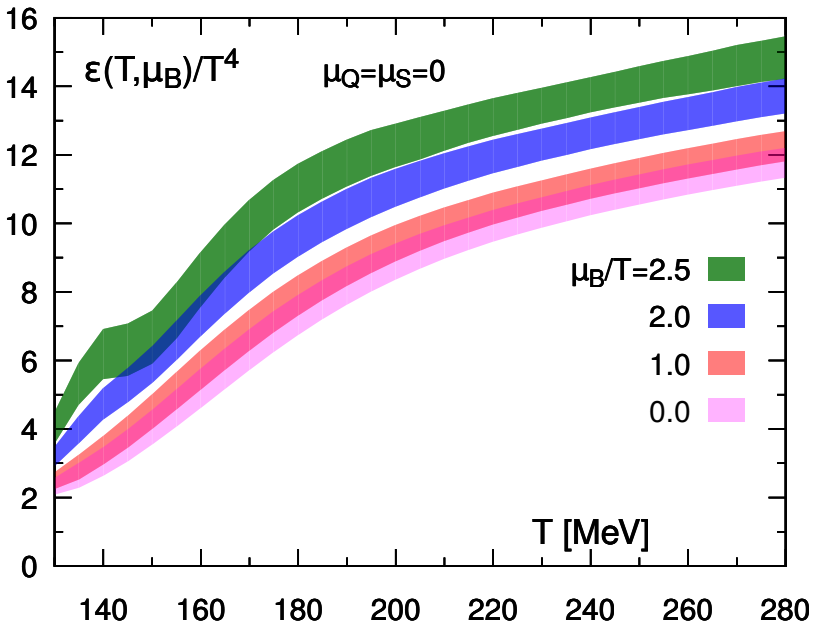

- The total pressure (left) and energy density (right) at various values of the baryon chemical potential

The equation of state at $O(\mu_B^6)$

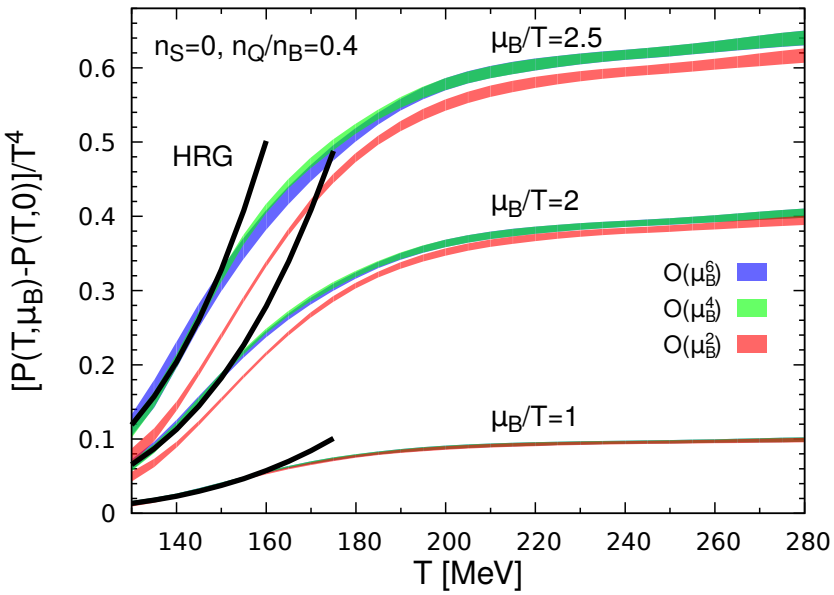

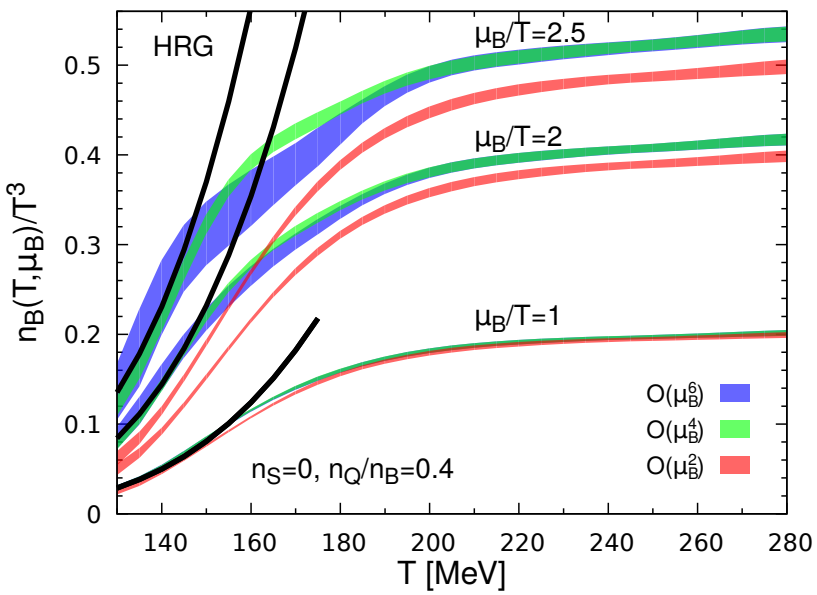

- The contribution to the pressure due to finite chemical potential (left) and the baryon number density (right) for strangeness neutral systems:

$$n_S = 0, \quad \frac{n_Q}{n_B} = 0.4$$

Constraints on the critical point

- For $\mu_Q = \mu_S = 0$ the net baryon-number susceptibility is

$$\chi_2^B(T, \mu_B) = \sum_{n=0}^{\infty} \frac{1}{(2n)!} \chi_{2n+2}^B \hat{\mu}_B^{2n}$$

Constraints on the critical point

- For $\mu_Q = \mu_S = 0$ the net baryon-number susceptibility is

$$\chi_2^B(T, \mu_B) = \sum_{n=0}^{\infty} \frac{1}{(2n)!} \chi_{2n+2}^B \hat{\mu}_B^{2n}$$

- The radius of convergence

$$r_{2n}^{\chi} \equiv \sqrt{\frac{2n(2n-1)\chi_{2n}^B}{\chi_{2n+2}^B}}$$

Constraints on the critical point

- For $\mu_Q = \mu_S = 0$ the net baryon-number susceptibility is

$$\chi_2^B(T, \mu_B) = \sum_{n=0}^{\infty} \frac{1}{(2n)!} \chi_{2n+2}^B \hat{\mu}_B^{2n}$$

- The radius of convergence

$$r_{2n}^{\chi} \equiv \sqrt{\frac{2n(2n-1)\chi_{2n}^B}{\chi_{2n+2}^B}}$$

- We observe $\chi_6^B/\chi_4^B < 3$ for $135 < T < 155$ MeV $\Rightarrow r_4^{\chi} \geqslant 2$

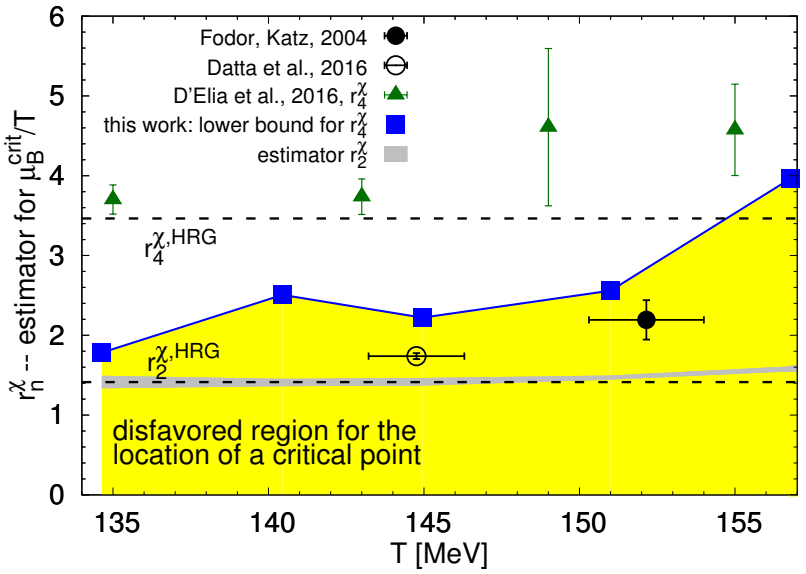

QCD phase diagram

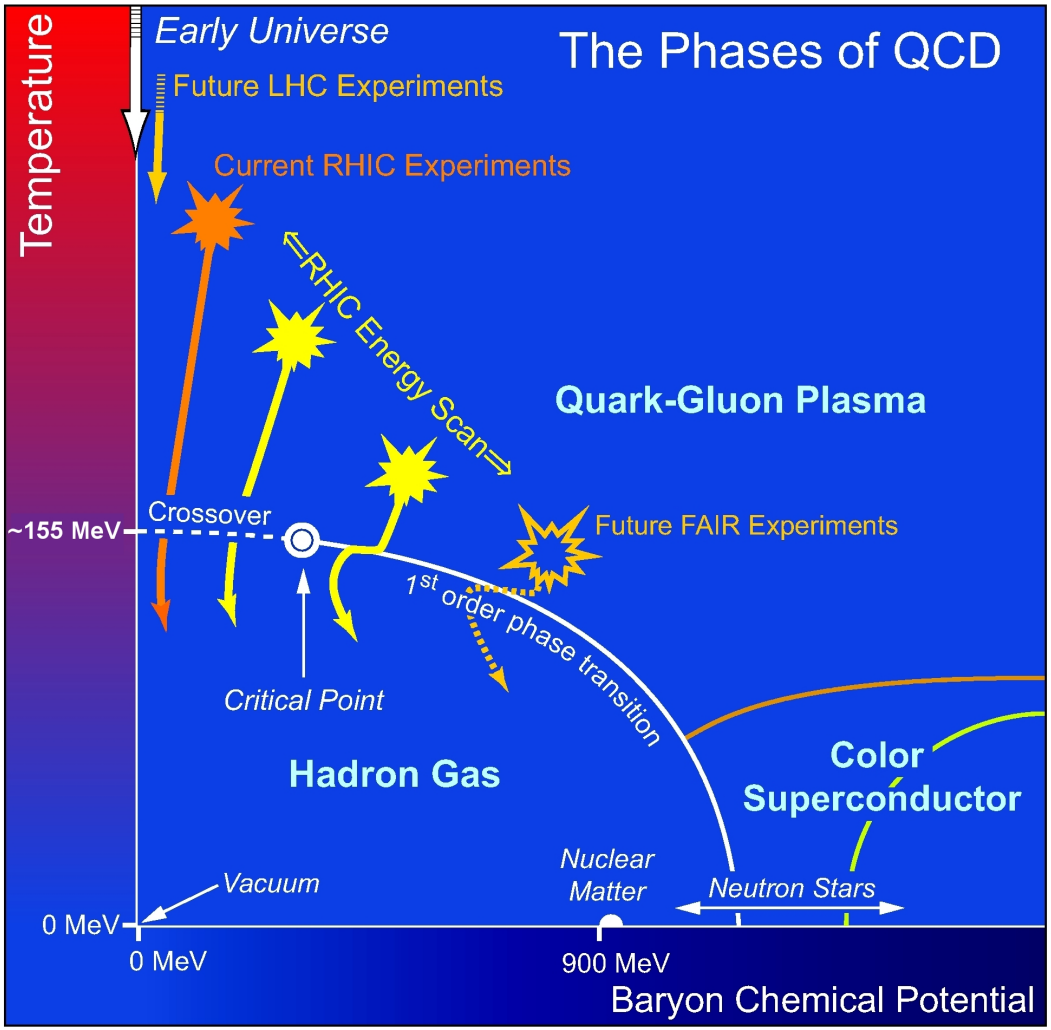

QCD phase diagram

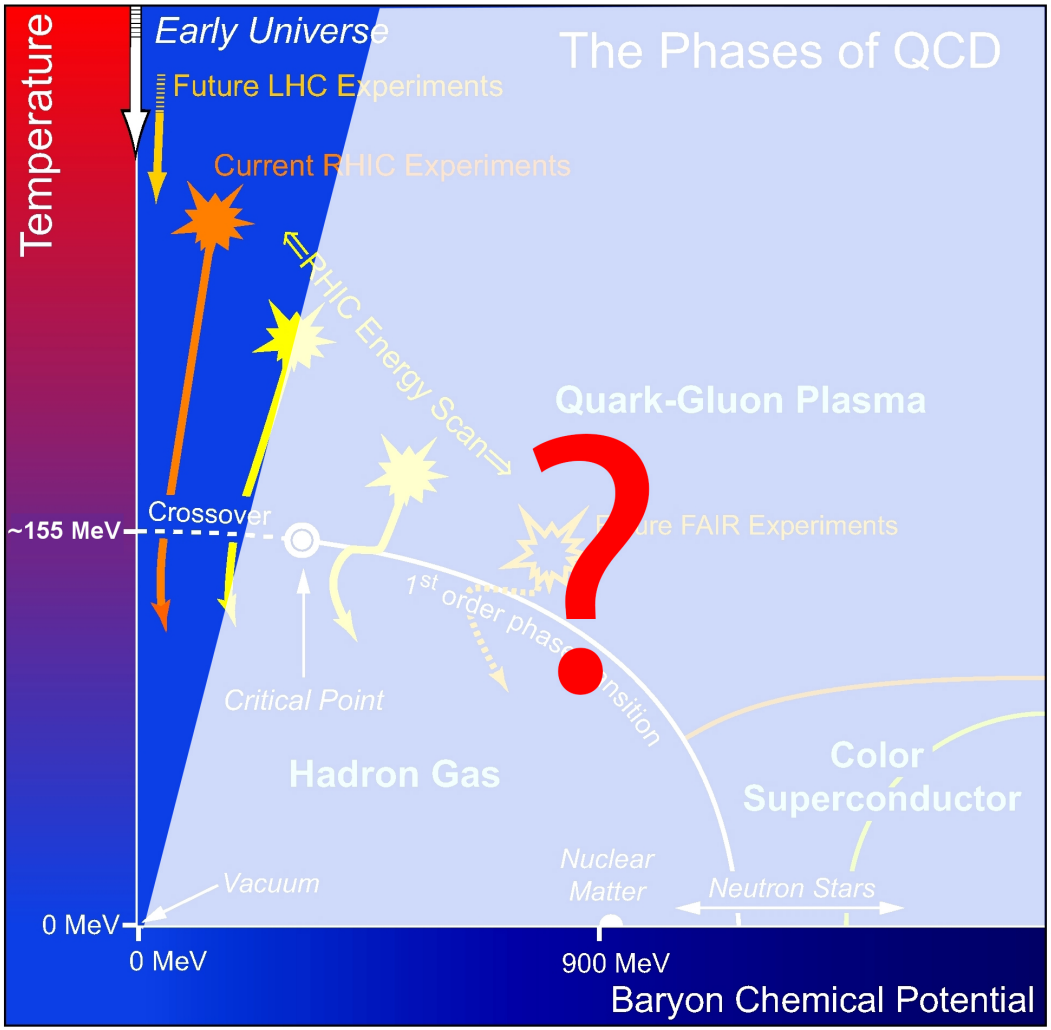

Conclusion

- Studying the QCD phase diagram requires non-perturbative tools, such as lattice QCD
- In recent years lattice simulations at the physical light quark mass with controlled systematic uncertainties became feasible
- At $\mu_B = 0$ the chiral crossover temperature is $T_c = 154(9)$ MeV
- The cumulants of conserved charges have been calculated on the lattice up to the sixth order
- Ratios of cumulants can be compared to the experimental measurements to determine the freeze-out parameters
- The QCD equation of state has been recently calculated up to $O(\mu_B^6)$
- The critical point is disfavored in the $135 < T < 155$ MeV range up to $\mu_B/T = 2$